Steel and Composite Structures, *Vol. 23, No. 3 (2017) 363-383*
DOI: https://doi.org/10.12989/scs.2017.23.3.363

Numerical investigation of web crippling strength in cold-formed stainless steel lipped channels with web openings subjected to interior-two-flange loading condition

Amir M. Yousefi [1a], Asraf Uzzaman [2b], James B.P. Lim [*1], G. Charles Clifton [1c] and Ben Young [3d]

[1] *Department of Civil and Environmental Engineering, The University of Auckland, New Zealand*
[2] *Department of Mechanical and Aerospace Engineering, The University of Strathclyde, 75 Montrose Street, Glasgow G1 1XJ, UK*
[3] *Department of Civil Engineering, The University of Hong Kong, Pokfulam Road, Hong Kong*

(*Received June 27, 2016, Revised December 14, 2016, Accepted January 17, 2017*)

Abstract. In cold-formed stainless steel lipped channel-sections, use of web openings for service purposes are becoming increasingly popular. Web openings, however, result in the sections becoming more susceptible to web crippling. This paper presents a finite element investigation into the web crippling strength of cold-formed stainless steel lipped channel-sections with circular web openings under the interior-two-flange (ITF) loading condition. The cases of web openings located centred and offset to the bearing plates are considered in this study. In order to take into account the influence of the circular web openings, a parametric study involving 2,220 finite element analyses was performed, covering duplex EN1.4462, austenitic EN1.4404 and ferritic EN1.4003 stainless steel grades. From the results of the parametric study, strength reduction factor equations are proposed. The strengths obtained from reduction factor equations are first compared to the strengths calculated from the equations recently proposed for cold-formed carbon steel lipped channel-sections. It is demonstrated that the strength reduction factor equations proposed for cold-formed carbon steel are unconservative for the stainless steel grades by up to 17%. New coefficients for web crippling strength reduction factor equations are then proposed that can be applied to all three stainless steel grades.

Keywords: cold-formed stainless steel; lipped channel-section; web crippling; finite element analysis; strength reduction factor

1. Introduction

The use of cold-formed stainless steel sections are growing in popularity for both architectural and structural applications. Not only they are aesthetically pleasing but they also have favourable characteristics in terms of strength, durability and formability (Rossi *et al*. 2009, Dai and Lam 2010, Kiymaz and Seckin 2014, Zhao *et al*. 2016). To provide ease of access for services, the use of web openings for such sections is also becoming popular in industry (Lawson *et al*. 2015) (see Fig. 1). Such web openings, however, result in the sections being more susceptible to web crippling, especially under concentrated loads in the vicinity of the openings.

The authors have recently proposed unified strength reduction factor equations for the web crippling strength of cold-formed stainless steel lipped channel-sections with circular web openings under the one-flange loading conditions (Yousefi *et al*. 2016a, b, c, d) and the two-flange loading conditions (Yousefi *et al*. 2016e, 2017). The equations covered three stainless steel grades; duplex grade EN 1.4462; austenitic grade EN 1.4404 and ferritic grade EN 1.4003. Similar equations for cold-formed carbon steel have previously been proposed by Lian *et al*. (2016a, b, 2017a, b), which was a continuation of the work conducted by Uzzaman *et al*. (2012a, b, c, 2013) who had considered the two-flange loading conditions. When applied to the stainless steel grades, Yousefi *et al*. (2016a, b, c, d) showed that the equations proposed by Lian *et al*. (2016a, b, 2017a, b) for the end-one-flange (EOF) loading condition were unconservative by up to 7%, and conservative for the interior-one-flange (IOF) loading condition by up to 9%.

In the literature, for cold-formed stainless steel lipped channel-sections, only Kroyink *et al*. (1996) has considered web crippling strength, but limited to sections without openings. Zhou and Young (2006, 2007, 2008, 2013) have considered the web crippling strength of cold-formed stainless steel tubular sections, again without openings. Keerthan and Mahendran (2012) and Keerthan *et al*. (2014) considered the web crippling strength of hollow flange channel beams, again without openings. Research by Lawson *et al*. (2015), while concerned with circular web openings, focussed on the bending strength of the sections and not on the web crippling strength under concentrated loads (see Fig. 1). For cold-formed carbon steel lipped

*Corresponding author, Senior Lecturer,
E-mail: james.lim@auckland.ac.nz
[a] Ph.D. Student, E-mail: ayou561@aucklanduni.ac.nz
[b] Research Fellow, E-mail: asraf.uzzaman@strath.ac.uk
[c] Associate Professor, E-mail: c.clifton@auckland.ac.nz
[d] Professor, E-mail: young@hku.hk

ISSN: 1229-9367 (Print), 1598-6233 (Online)

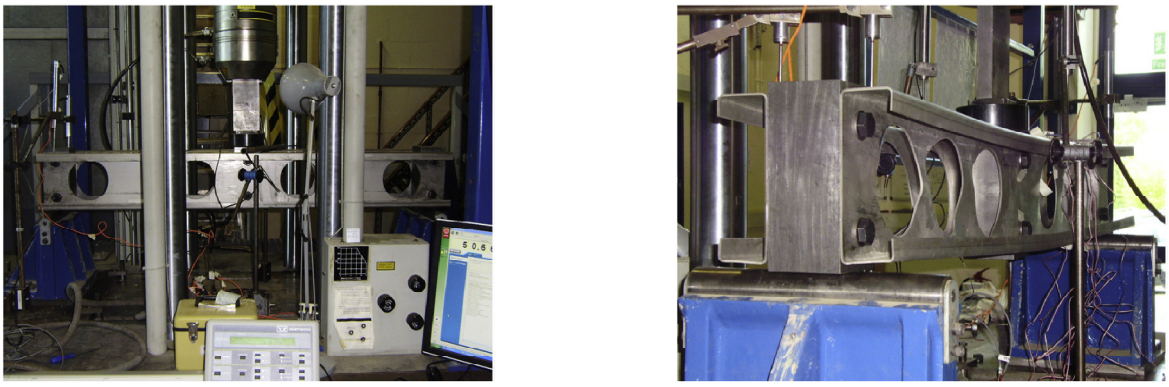

Fig. 1 Photograph of cold-formed stainless steel lipped channel-sections with circular web openings after Lawson *et al*. (2015)

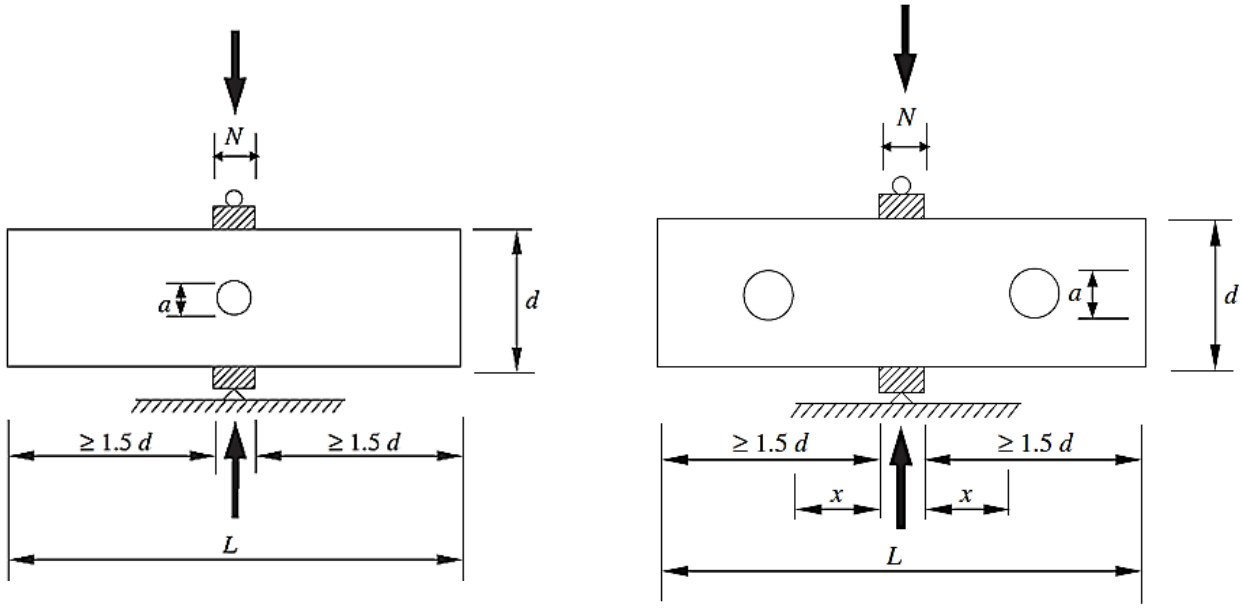

(a) With circular web opening centred under bearing plate

(b) With circular web openings offset from bearing plate

Fig. 2 Interior-two-flange (ITF) loading condition after Uzzaman *et al*. (2012a, b)

(a) Centred circular web opening

(b) Offset circular web opening

Fig. 3 Experimental analysis of cold-formed steel lipped channel-sections under interior-two-flange (ITF) loading condition for the case of flange unfastened to bearing plate after Uzzaman *et al*. (2012a, b)

channel-sections, recent work has included Natário *et al*. (2014), Chen *et al*. (2015) and Gunalan and Mahendran (2015), all without openings.

This paper considers the case of the web crippling strength of cold-formed stainless steel lipped channel-sections with circular web openings under the interior-two-

flange (ITF) loading condition (see Figs. 2 and 3), and applicability of the proposed equations by Uzzaman *et al*. (2012a, c) to the same three stainless steel grades i.e. duplex grade EN 1.4462; austenitic grade 1.4404 and ferritic grade 1.4003. In this study, stress-strain curves for the three stainless steel grades were obtained from Chen and Young (2006) and Arrayago *et al*. (2015).

2. Experimental investigation

For cold-formed carbon steel, Uzzaman *et al*. (2012a, b) recently conducted 75 interior-two-flange (ITF) laboratory tests on lipped channel-sections with circular web openings subjected to web crippling (see Fig. 3). The size of the circular web openings was varied in order to investigate the effect of the web openings on the web crippling strength. All the test specimens were fabricated with web openings located at the mid-depth of the webs with the web openings centred and offset to the bearing plates. The laboratory test results were used to validate a non-linear geometry elasto-plastic finite element model (details of the model can be found in Uzzaman *et al*. (2012a, b)), which was then used for a parametric study to investigate the web crippling strength of cold-formed stainless steel lipped channel-sections with circular web openings under the interior-two-flange (ITF) loading condition. Recommendations are proposed in the form of strength reduction factor equations, relating the loss of strength due to the web openings to the strength of the web without openings. The size of the circular web openings was varied in order to investigate the effect of the web opening size on the web crippling strength. Full details of both the laboratory tests can be found in Uzzaman *et al*. (2012a, b).

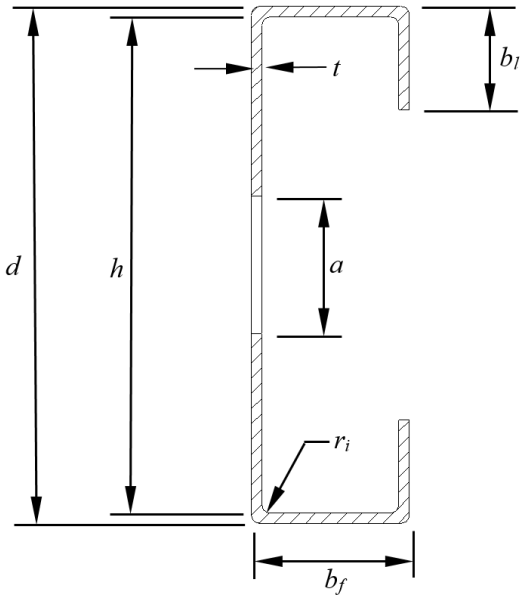

Fig. 4 Definition of symbols

3. Numerical investigation

3.1 General

In this study, the non-linear elasto-plastic general purpose finite element program ABAQUS (2014) was used to simulate the cold-formed stainless steel lipped channel sections with and without circular web openings subjected to web crippling. The bearing plates, the lipped channel-section with circular web openings and the interfaces between the bearing plates and the lipped-channel section have been modelled. In the finite element model, the model was based on the centreline dimensions of the cross-sections. Details of the finite element models in ABAQUS (2014) are summarised below.

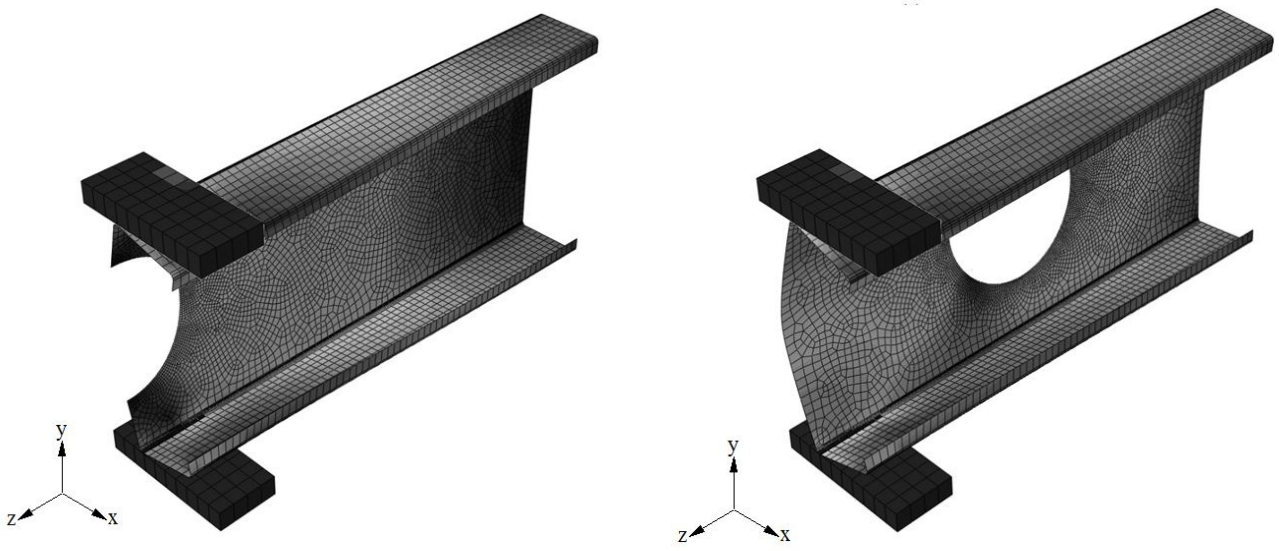

(a) Centred circular web opening

(b) Offset circular web opening

Fig. 5 Deformed shape predicted from finite element analysis of cold-formed steel lipped channel-sections under interior-two-flange (ITF) loading condition for case of flange unfastened to bearing plate

Table 1 Dimensions and web crippling strengths predicted from finite element analysis of cold-formed stainless steel lipped channel-sections

A. For the case of flange unfastened to the bearing plate

Specimen	Web	Flange	Lip	Thickness	Length	Web opening	Duplex			Ferritic			Austenitic		
	d (mm)	b_f (mm)	b_l (mm)	t (mm)	L (mm)	a (mm)	$P(A0)$ (kN)	$P(Opening)$ (kN)	$P(Opening)$ (kN)	$P(A0)$ (kN)	$P(Opening)$ (kN)	$P(Opening)$ (kN)	$P(A0)$ (kN)	$P(Opening)$ (kN)	$P(Opening)$ (kN)
								Offset	Centred		Offset	Centred		Offset	Centred
142-N100-MA0.6-FR	141.82	60.63	13.66	1.27	720.00	139.27	6.95	5.67	5.86	6.29	5.09	5.34	5.77	4.56	4.87
142-N120-MA0.6-FR	142.24	60.37	13.90	1.27	740.00	139.70	7.50	6.07	6.33	6.63	5.45	5.63	6.26	4.98	5.36
142-N150-MA0.4-FR	142.40	59.79	13.28	1.28	770.00	139.84	7.82	7.13	6.97	7.05	6.45	6.30	6.44	5.84	5.79
202-N100-MA0.4-FR	202.04	64.79	14.78	1.38	899.20	199.28	6.56	5.63	5.84	6.08	5.37	5.42	5.78	5.02	5.13
202-N100-MA0.6-FR	202.04	64.79	14.78	1.38	899.20	199.28	6.56	5.23	5.42	6.08	4.95	5.04	5.78	4.58	4.76
202-N120-MA0.4-FR	202.00	65.00	14.73	1.38	920.00	199.24	6.82	5.97	6.09	6.34	5.62	5.63	6.04	5.43	5.35
202-N120-MA0.6-FR	202.00	65.00	14.73	1.38	920.00	199.24	6.82	5.56	5.63	6.34	5.19	5.24	6.04	4.98	4.96
202-N150-MA0.4-FR	202.01	65.04	14.98	1.38	950.00	199.24	7.28	6.27	5.41	6.78	6.06	5.11	6.48	5.84	4.94
302-N100-MA0.6-FR	303.18	87.91	18.83	1.90	1200.00	299.37	12.08	10.16	9.73	11.53	10.66	9.34	11.19	10.55	9.11
302-N120-MA0.6-FR	303.07	87.95	18.26	1.90	1221.00	299.26	12.34	10.79	9.89	11.77	11.34	9.48	11.46	11.25	9.27
302-N150-MA0.6-FR	303.03	88.54	18.97	1.90	1249.00	299.23	20.39	15.25	10.29	19.76	15.01	10.08	20.04	14.92	10.05

B. For the case of flange fastened to the bearing plate

Specimen	Web	Flange	Lip	Thickness	Length	Web opening	Duplex			Ferritic			Austenitic		
	d (mm)	b_f (mm)	b_l (mm)	t (mm)	L (mm)	a (mm)	$P(A0)$ (kN)	$P(Opening)$ (kN)	$P(Opening)$ (kN)	$P(A0)$ (kN)	$P(Opening)$ (kN)	$P(Opening)$ (kN)	$P(A0)$ (kN)	$P(Opening)$ (kN)	$P(Opening)$ (kN)
								Offset	Centred		Offset	Centred		Offset	Centred
142-N100-MA0.6-FX	142.49	60.33	13.79	1.29	720.00	139.27	11.31	9.65	7.14	9.65	8.57	6.21	8.97	7.80	5.72
142-N120-MA0.6-FX	142.38	60.21	13.68	1.29	740.00	139.70	10.06	9.98	7.56	10.04	8.83	6.56	9.37	8.09	6.00
142-N150-MA0.4-FX	142.18	60.12	13.19	1.28	770.00	139.84	12.18	10.82	8.91	10.55	9.57	7.62	9.47	8.72	7.00
202-N100-MA0.4-FX	201.99	64.87	14.76	1.37	900.00	199.28	12.24	11.79	7.50	10.65	10.63	6.71	10.55	9.94	6.29
202-N100-MA0.6-FX	201.99	64.87	14.76	1.37	900.00	199.28	12.24	11.07	7.06	10.65	9.89	6.32	10.55	9.51	5.91
202-N120-MA0.4-FX	202.05	64.99	14.82	1.41	920.00	199.24	13.46	11.32	8.43	12.01	10.22	7.51	10.47	9.70	7.02
202-N120-MA0.6-FX	202.05	64.99	14.82	1.41	920.00	199.24	13.46	10.69	7.95	12.01	9.63	7.07	10.47	9.26	6.58
202-N150-MA0.4-FX	202.00	64.93	15.00	1.41	950.00	199.24	13.81	12.52	9.10	12.44	11.27	8.07	11.67	10.75	7.53
302-N100-MA0.6-FX	303.20	88.24	18.66	1.96	1199.00	299.37	24.65	21.44	12.31	20.83	19.39	11.48	19.24	18.31	11.12
302-N120-MA0.6-FX	303.50	88.53	18.36	1.93	1219.00	299.26	24.54	21.26	13.35	21.70	19.64	12.38	19.86	18.89	11.94
302-N150-MA0.6-FX	303.85	88.71	18.41	1.90	1248.33	299.23	24.36	23.68	14.04	22.42	21.44	12.99	28.56	27.19	12.57

Table 2 Comparison of numerical results with design strength for the case of flange unfastened to the bearing plate without circular web opening

Specimen	Web slenderness	Bearing length to thickness ratio	Bearing length to web height ratio	Inside bend radius ratio	Failure load per web	Web crippling strength per web predicted from current design codes					Comparison				
	h/t	N/t	N/h	r_i/t	P_{FEA} (kN)	P_{NAS} (kN)	P_{ASCE} (kN)	P_{BS} (kN)	P_{Euro} (kN)	$P_{AS/NZS}$	P/P_{NAS}	P/P_{ASCE}	$P/P_{AS/NZS}$	P/P_{BS}	P/P_{Euro}
142-N100	109.67	78.74	0.72	3.78	5.77	5.35	5.36	6.33	4.84	5.36	1.08	1.08	1.08	0.91	1.19
142-N120	110.00	94.49	0.86	3.78	6.05	5.63	5.94	6.73	5.36	5.94	1.07	1.02	1.07	0.90	1.13
142-N150	109.25	117.19	1.07	3.75	6.44	6.12	6.89	6.77	6.22	6.89	1.05	0.93	1.05	0.95	1.04
202-N100	144.41	72.46	0.50	3.62	5.61	6.28	5.88	6.53	5.31	5.88	0.89	0.95	0.89	0.86	1.06
202-N120	144.38	86.96	0.60	3.62	6.04	6.61	6.49	6.64	5.85	6.49	0.91	0.93	0.91	0.91	1.03
202-N150	144.38	108.70	0.75	3.62	7.09	7.05	7.40	6.81	6.68	7.40	1.01	0.96	1.01	1.04	1.06
302-N100	157.57	52.63	0.33	2.63	11.19	12.74	10.92	12.66	9.85	10.92	0.88	1.02	0.88	0.88	1.14
302-N120	157.51	63.16	0.40	2.63	11.46	13.35	11.53	12.81	10.40	11.53	0.86	0.99	0.86	0.89	1.10
302-N150	155.01	77.72	0.50	2.59	19.19	14.31	13.00	13.05	11.74	13.00	1.34	1.48	1.34	1.47	1.64
Mean, Pm											1.01	1.04	1.01	0.98	1.15
Coefficient of variation											0.15	0.16	0.15	0.2	0.16

3.2 Specimens labelling

The dimensions of the lipped channel-section modelled are given in Table 1. Fig. 4 shows the definition of the symbols used to describe the dimensions of the cold-formed carbon steel lipped channel-sections considered in the test programme. The models have been coded such the nominal dimension of the model and the length of the bearing plate as well as the ratio of the diameter of the circular web openings to the depth of the flat portion of the webs (a/h) can be determined from the coding system. As an example, the label "142-N100-A0.2-FR" means the following. The first notation is the nominal depth of the models in millimeters. The notation "*N100*" indicates the length of bearing in millimeters (i.e., 100 mm). The notation "*A*0.2" indicates the ratio of the diameter of the openings to the depth of the flat portion of the webs (a/h) and are one of 0.2, 0.4, 0.6 and 0.8 (i.e., *A*0.2 means a/h = 0.2; *A*0.4 means a/h = 0.4 etc). Plain lipped channel-sections (i.e., without circular web openings) are denoted by "*A*0". The flange unfastened and fastened cases are identified as "*FR*" and "*FX*", respectively.

3.3 Geometry and material properties

In the finite element model, half of the test set-up of Uzzaman *et al*. (2012a, b) was modelled using symmetry about the vertical transverse plane, as shown in Fig. 5. The stress-strain curves for duplex grade EN 1.4462; austenitic grade 1.4404 and ferritic grade 1.4003 were obtained from Chen and Young (2006) and Arrayago *et al*. (2015). The stress-strain curves were converted into true stress-strain curves as per the equations described in the ABAQUS manual (2014). Comparative hot-rolled steel stress strain curves can be found in Yousefi *et al*. (2014) and Rezvani *et al*. (2015).

3.4 Element type and mesh sensitivity

Fig. 5 shows details of a typical finite element mesh of the channel section and the bearing plate. The effect of different element sizes in the cross-section of the channel section was investigated to provide both accurate results and reduced computation time. Finite element mesh sizes were 10 mm × 10 mm for the cold-formed steel channel sections and 18 mm × 18 mm for the bearing plates.

Cold-formed steel lipped channel-sections with and without web openings were modelled using S4R shell element. The S4R is a four-node double curved thin or thick shell element with reduced integration and finite membrane strains. It is mentioned in the ABAQUS Manual (2014) that the S4R element is suitable for complex buckling behaviour. The S4R has six degrees of freedom per node and provides accurate solutions to most applications. The bearing plates and load transfer block were modelled using analytical rigid plates and C3D8R element, which is suitable for three-dimensional modelling of structures with plasticity, stress stiffening, large deflection, and large strain capabilities. The solid element is defined by eight nodes having three translational degrees of freedom at each node.

3.5 Loading and boundary conditions

Contact between the bearing plate and the cold-formed stainless steel section was modelled in ABAQUS using the *contact pairs* option. The interface between the bearing plates and the cold-formed stainless steel section were modelled using the *surface-to-surface contact* option. The bearing plates were the master surface, while the flange of the cross-section of stainless steel section was the slave surface extended up to the corners. The two contact surfaces were not allowed to penetrate each other. The vertical load applied to the channel sections in the laboratory tests was modelled using displacement control method; an imposed displacement is applied to the nodes of the top bearing plate where the vertical load is applied. The top bearing plate was restrained against all degrees of freedom, except for the translational degree of freedom in the Y direction. In the flanges fastened condition, the node coupling method was used in the region where the flanges connected to the

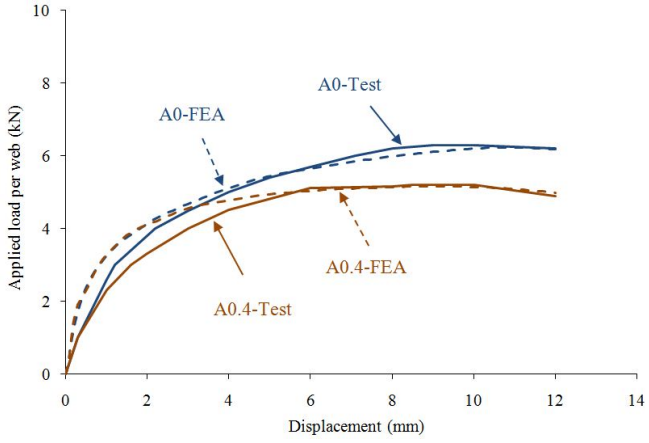

(a) Offset circular web opening for the case of flange unfastened to bearing plate

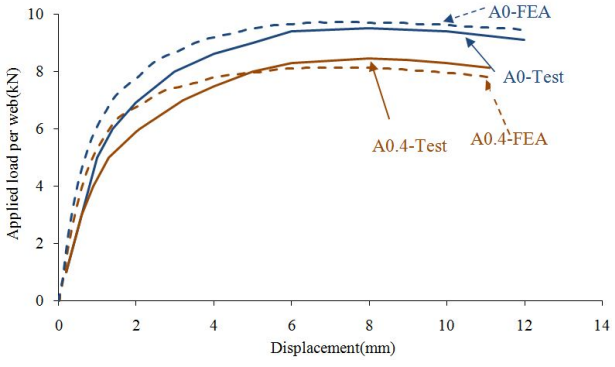

(b) Offset circular web opening for the case of flange fastened to bearing plate

Fig. 6 Comparison of finite element results and experimental test results Uzzaman *et al*. (2012a, b)

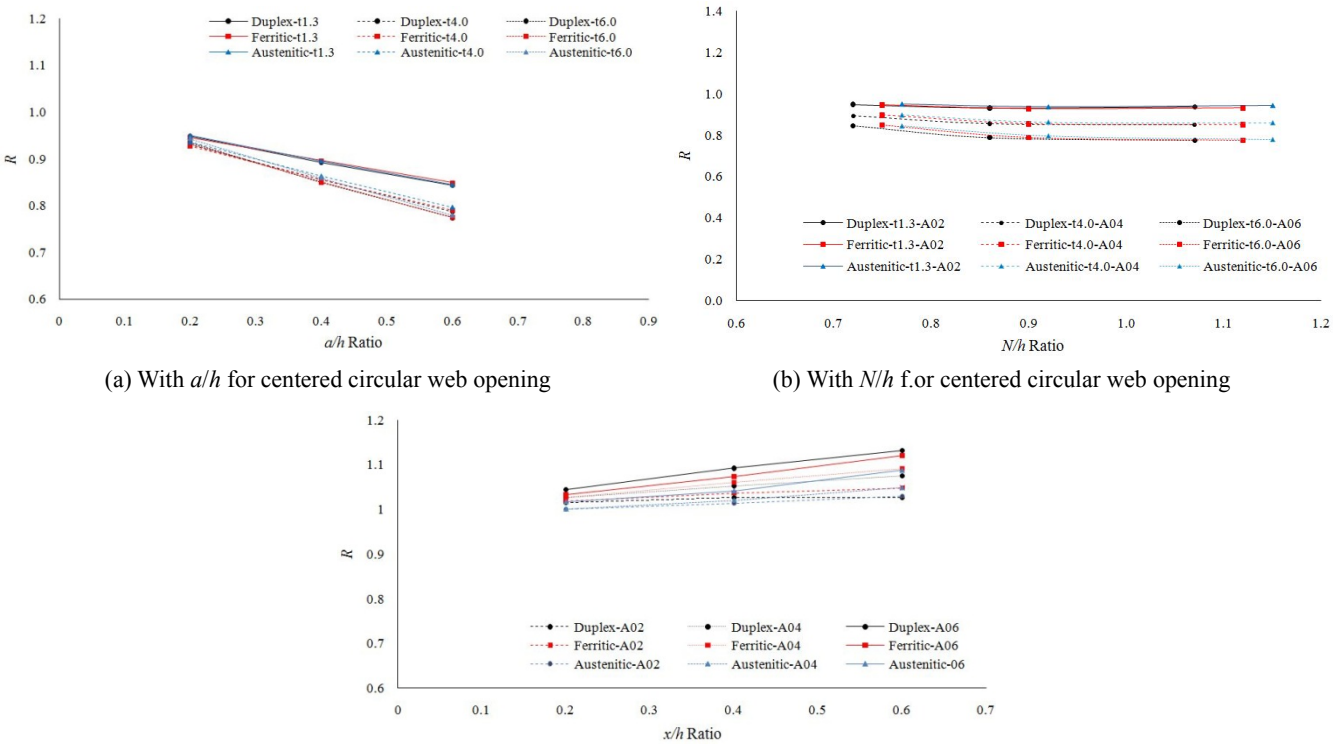

(a) With *a*/*h* for centered circular web opening

(b) With *N*/*h* f.or centered circular web opening

(c) With *x*/*h* for offset circular web opening

Fig. 7 Variation in reduction factors for C142 section for the case of flange unfastened to bearing plate

bearing plates. The nodes were coupled together in all degrees of freedom.

3.6 Verification of finite element model

In order to verify the finite element model, the results of experimental study on lipped carbon steel channel sections 172×65×13-t1.3-N65-FR and 172×65×13-t1.3-N65-FX under ITF loading condition conducted by Uzzaman *et al*. (2012a, b) (see Fig. 3) were compared to the results obtained from the finite element analyses (Fig. 6) using the same material as developed for stainless steel materials in this study. As can be seen, there is good agreement between the failure loads of the tested specimens and the finite element results. For cold-formed stainless steel lipped channel-sections, the numerical failure loads with and without circular web openings were then determined for the three stainless steel grades: duplex grade EN 1.4462; austenitic grade 1.4404 and ferritic grade 1.4003 (see Table 1). These results were compared with the failure loads calculated in accordance with ASCE 8-02 (2002), BS 5950-5 (1998), Eurocode-3 (2006), NAS (2007) and AS/NZS 4600 (2005) (see Table 2). The failure loads predicted from the finite element model are similar to the codified failure loads of the sections.

4. Parametric study for stainless steel grades

In order to investigate the effect of circular web openings on the web crippling strength of cold-formed stainless steel lipped channel-sections, a total of 2,220 finite element analyses using the verified FE model of lipped channel-sections with various dimensions and thicknesses were considered for three stainless steel grades: duplex EN1.4462, austenitic EN1.4404 and ferretic EN1.4003.

Previous work by Uzzaman *et al*. (2012a, b) on carbon steel showed that the web crippling strengths of cold-formed stainless steel lipped channel-sections with circular web openings were affected primarily by the web opening diameter (*a*), length of bearing plate (*N*) and location of web openings in the web (*x*). Tables 3 to 5 show the web crippling strengths determined from finite element analyses for the duplex grade EN 1.4462, austenitic grade 1.4404 and ferritic grade 1.4003. The web crippling strengths for sections with circular web openings were divided by that for sections without web openings and considered as the strength reduction factor (*R*).

Fig. 7(a) shows the ratio of the circular web opening depth to the flat portion of the web (*a*/*h*) versus the strength reduction factor, for the three stainless steel grades. As can be seen, the strength reduction factor decreases as the parameter *a*/*h* increases for all three stainless steels, in particular for the ferritic grade with higher thickness (6.0 mm). The reduction in strength of the ferritic grade 1.3 mm thick section is smallest and the strength reduction factor decreases as the section becomes thinner. It can be seen that when the *a*/*h* ratio increases from 0.2 to 0.6, the strength reduction factor decreases for the ferritic grade increases by 23%.

Fig. 7(b) shows the ratio of the bearing length to the flat portion of the web (*N*/*h*) versus the strength reduction factor, for the three stainless steel grades. As can be seen, the strength reduction factor is not sensitive to the ratio *N*/*h*

Table 3 Web crippling strengths of duplex stainless steel sections predicted from finite element analysis

A. *a*/*h* for centred circular web opening case

Specimen	Thickness	Unfastened FEA load per web, P_{FEA}					Fastened FEA load per web, P_{FEA}				
	t	*A*(*0*)	*A*(*0.2*)	*A*(*0.4*)	*A*(*0.6*)	*A*(*0.8*)	*A*(*0*)	*A*(*0.2*)	*A*(*0.4*)	*A*(*0.6*)	*A*(*0.8*)
	(*mm*)	(*kN*)	(*kN*)	(*kN*)	(*kN*)	(*kN*)	(*kN*)	(*kN*)	(*kN*)	(*kN*)	(*kN*)
142-N100-FR	1.27	6.95	6.58	6.20	5.86	-	11.31	7.91	7.52	7.14	-
142-N100-FR	4.00	79.00	73.41	67.48	62.13	-	113.38	95.83	88.55	81.99	-
142-N100-FR	6.00	188.38	176.11	160.06	145.77	-	256.16	222.77	205.31	188.85	-
142-N120-FR	1.27	7.50	7.11	6.71	6.33	5.96	11.60	8.40	7.96	7.56	7.10
142-N120-FR	4.00	85.25	79.28	72.70	66.96	61.68	118.83	103.41	95.45	88.01	80.54
142-N120-FR	6.00	203.09	189.28	173.19	157.65	143.49	272.25	241.84	222.90	204.61	183.37
142-N150-FR	1.28	7.82	7.40	6.97	6.58	6.20	12.18	9.35	8.91	8.49	7.99
142-N150-FR	4.00	92.11	85.79	79.01	72.56	66.91	128.01	115.42	107.15	99.44	91.28
142-N150-FR	6.00	219.95	206.10	189.69	173.94	158.70	296.54	271.01	252.04	234.01	213.41
202-N100-FR	1.39	6.56	6.25	5.84	5.42	-	12.24	7.97	7.50	7.06	-
202-N100-FR	4.00	67.74	62.76	57.15	52.17	-	115.51	87.94	81.17	74.93	-
202-N100-FR	6.00	166.19	154.14	138.56	124.52	-	256.13	209.76	192.70	176.84	-
202-N120-FR	1.39	6.82	6.49	6.06	5.63	-	13.46	8.95	8.43	7.95	-
202-N120-FR	4.00	71.21	66.04	60.03	54.71	-	120.68	93.61	86.19	79.45	-
202-N120-FR	6.00	175.98	163.05	146.55	131.68	-	273.75	225.77	206.97	189.82	-
202-N150-FR	1.39	7.28	6.82	5.41	4.95	-	13.81	9.64	9.10	8.59	-
202-N150-FR	4.00	77.13	71.42	63.75	57.86	-	124.91	102.48	94.12	86.48	-
202-N150-FR	6.00	188.24	177.08	158.02	142.00	-	290.41	248.96	228.15	209.03	-
302-N100-FR	1.98	12.08	11.55	10.61	9.73	-	24.65	15.48	14.70	12.31	-
302-N100-FR	4.00	58.94	55.24	50.56	46.31	-	107.14	73.27	66.98	61.02	-
302-N100-FR	6.00	145.14	134.80	120.86	120.87	-	246.08	180.07	163.85	148.88	-
302-N120-FR	1.98	12.34	11.77	10.82	9.89	-	24.54	16.07	14.00	13.35	-
302-N120-FR	4.00	60.65	56.71	51.96	47.46	-	111.34	75.96	69.38	62.97	-
302-N120-FR	6.00	150.92	139.52	124.91	112.80	-	257.03	188.50	170.90	154.51	-
302-N150-FR	1.99	20.39	13.64	12.01	10.29	-	24.36	17.10	14.70	14.04	-
302-N150-FR	4.00	91.20	59.80	53.84	48.57	-	113.59	80.49	73.25	66.53	-
302-N150-FR	6.00	212.06	151.69	135.10	120.87	-	264.67	201.17	181.83	163.99	-

B. *a*/*h* for offset circular web opening case

Specimen	Thickness	Unfastened FEA load per web, P_{FEA}				Fastened FEA load per web, P_{FEA}			
	t	*A*(*0*)	*A*(*0.2*)	*A*(*0.4*)	*A*(*0.6*)	*A*(*0*)	*A*(*0.2*)	*A*(*0.4*)	*A*(*0.6*)
	(*mm*)	(*kN*)	(*kN*)	(*kN*)	(*kN*)	(*kN*)	(*kN*)	(*kN*)	(*kN*)
142-N100-FR	1.27	6.95	6.53	6.07	5.67	11.46	10.96	10.29	9.65
142-N100-FR	4.00	79.00	76.64	73.02	69.61	113.05	111.47	109.31	107.49
142-N100-FR	6.00	188.38	184.65	177.58	169.22	255.93	254.59	251.93	249.08
142-N120-FR	1.27	7.02	6.61	6.59	6.07	11.72	11.23	10.56	9.98
142-N120-FR	4.00	84.49	82.17	78.48	74.94	118.40	117.14	115.20	113.38
142-N120-FR	6.00	200.02	197.87	190.06	182.21	272.42	270.64	267.75	264.55
142-N150-FR	1.28	7.82	7.53	7.13	6.61	11.91	11.44	10.82	10.30
142-N150-FR	4.00	92.11	89.75	85.98	82.40	127.22	126.16	124.35	122.56
142-N150-FR	6.00	219.95	215.46	207.85	200.02	295.89	294.33	291.27	287.47
202-N100-FR	1.39	6.35	6.03	5.63	5.23	13.15	12.64	11.79	11.07
202-N100-FR	4.00	67.74	65.29	62.05	59.12	117.60	114.65	111.11	108.56

B. Continued

Specimen	Thickness	Unfastened FEA load per web, P_{FEA}				Fastened FEA load per web, P_{FEA}			
	t	*A*(*0*)	*A*(*0.2*)	*A*(*0.4*)	*A*(*0.6*)	*A*(*0*)	*A*(*0.2*)	*A*(*0.4*)	*A*(*0.6*)
	(*mm*)	(*kN*)	(*kN*)	(*kN*)	(*kN*)	(*kN*)	(*kN*)	(*kN*)	(*kN*)
202-N100-FR	6.00	166.19	162.37	155.14	148.64	261.84	260.34	257.34	254.24
202-N120-FR	1.39	6.82	6.38	5.97	5.56	12.64	12.12	11.32	10.69
202-N120-FR	4.00	71.21	69.07	65.95	63.08	120.73	118.07	114.82	112.47
202-N120-FR	6.00	175.98	172.03	165.59	159.04	274.17	251.88	268.82	265.30
202-N150-FR	1.39	7.10	6.83	6.27	5.99	13.81	13.24	12.52	11.92
202-N150-FR	4.00	77.12	75.18	70.97	69.21	125.01	123.01	120.47	118.48
202-N150-FR	6.00	191.02	187.42	178.44	174.32	291.03	289.11	285.78	282.42
302-N100-FR	1.98	11.02	10.71	10.23	10.16	24.65	23.97	22.70	21.44
302-N100-FR	2.00	58.96	56.34	52.49	48.98	107.15	104.53	99.69	95.16
302-N100-FR	4.00	145.33	141.02	134.54	128.51	246.16	243.32	237.15	231.29
302-N120-FR	1.98	11.24	11.04	10.84	10.79	24.54	23.76	22.54	21.26
302-N120-FR	2.00	60.65	58.20	54.52	51.19	111.36	107.42	101.47	97.33
302-N120-FR	4.00	150.92	147.05	140.93	134.92	257.21	251.88	244.55	226.42
302-N150-FR	1.99	18.56	17.81	16.29	15.25	26.94	23.77	22.56	23.68
302-N150-FR	2.00	91.20	86.20	78.85	69.2	113.63	109.51	104.33	97.76
302-N150-FR	4.00	212.06	201.35	195.45	168.3	264.67	260.28	241.93	241.65

C. *x*/*h* for offset circular web opening case

Specimen	Thickness	Unfastened FEA load per web, $P_{(FEA)}$				Fastened FEA load per web, P_{FEA}			
	t	*X*(*0*)	*X*(*0.2*)	*X*(*0.4*)	*X*(*0.6*)	*X*(*0*)	*X*(*0.2*)	*X*(*0.4*)	*X*(*0.6*)
	(*mm*)	(*kN*)	(*kN*)	(*kN*)	(*kN*)	(*kN*)	(*kN*)	(*kN*)	(*kN*)
142-N100-A0-FR	1.27	6.92	6.92	6.92	6.92	11.40	11.40	11.40	11.40
142-N100-A0.2-FR	1.27	6.32	6.41	6.48	6.54	10.66	10.69	10.78	11.40
142-N100-A0.4-FR	1.27	5.68	5.83	5.98	6.11	9.48	9.75	10.00	10.26
142-N100-A0.6-FR	1.27	5.01	5.23	5.47	5.67	8.20	8.75	9.20	9.63
142-N100-A0.8-FR	1.27	4.24	4.40	4.72	4.98	6.91	8.03	8.36	8.67
142-N120-A0-FR	1.27	7.26	7.26	7.26	7.26	11.67	11.67	11.67	11.67
142-N120-A0.2-FR	1.27	6.32	6.81	6.91	7.01	10.95	10.99	11.08	11.19
142-N120-A0.4-FR	1.27	6.07	6.24	6.43	6.61	9.76	10.04	10.29	10.54
142-N120-A0.6-FR	1.27	5.47	5.67	5.88	6.04	8.52	9.05	10.29	9.91
142-N120-A0.8-FR	1.27	4.72	4.39	5.15	5.39	7.33	8.11	8.76	9.34
142-N150-A0-FR	1.28	7.72	7.72	7.72	7.72	11.87	11.87	11.87	11.87
142-N150-A0.2-FR	1.28	7.19	7.31	7.41	7.48	11.14	11.20	11.29	11.41
142-N150-A0.4-FR	1.28	6.57	6.77	6.94	7.11	10.02	10.02	10.29	10.77
142-N150-A0.6-FR	1.28	5.98	6.22	6.41	6.58	8.90	9.39	9.81	10.21
142-N150-A0.8-FR	1.28	5.30	5.59	5.80	6.02	7.85	8.59	9.22	9.75
202-N100-A0-FR	1.39	6.52	6.52	6.52	6.52	12.63	12.63	12.63	12.63
202-N100-A0.2-FR	1.39	6.03	6.09	6.12	6.18	11.89	11.90	12.01	12.15
202-N100-A0.4-FR	1.39	5.30	5.44	5.58	5.74	10.30	10.62	10.99	11.35
202-N100-A0.6-FR	1.39	4.57	4.84	5.08	5.33	8.71	9.36	10.01	10.57
202-N120-A0-FR	1.39	6.79	6.79	6.79	6.79	12.94	12.94	12.94	12.94
202-N120-A0.2-FR	1.39	6.32	6.34	6.38	6.44	12.14	12.17	12.30	12.43
202-N120-A0.4-FR	1.39	5.55	5.71	5.85	6.02	10.54	10.89	11.24	11.59
202-N120-A0.6-FR	1.39	4.98	5.10	5.34	5.59	9.04	9.71	10.35	10.90

C. Continued

Specimen	Thickness	Unfastened FEA load per web, $P_{(FEA)}$				Fastened FEA load per web, P_{FEA}			
	t	$X(0)$	$X(0.2)$	$X(0.4)$	$X(0.6)$	$X(0)$	$X(0.2)$	$X(0.4)$	$X(0.6)$
	(mm)	(kN)	(kN)	(kN)	(kN)	(kN)	(kN)	(kN)	(kN)
202-N150-A0-FR	1.45	7.87	7.87	7.87	7.87	14.61	14.61	14.61	14.61
202-N150-A0.2-FR	1.45	7.40	7.46	7.51	7.58	13.64	13.72	13.86	14.02
202-N150-A0.4-FR	1.45	6.60	6.79	6.95	7.13	11.98	12.37	12.78	13.14
202-N150-A0.6-FR	1.45	5.81	6.11	6.39	6.68	10.47	11.23	11.93	12.51
302-N100-A0-FR	1.98	12.24	12.24	12.24	12.24	24.36	24.36	24.36	24.36
302-N100-A0.2-FR	1.98	11.28	11.53	11.82	11.88	23.19	23.22	23.52	23.78
302-N120-A0-FR	1.96	12.19	12.19	12.19	12.19	24.39	24.39	24.39	24.39
302-N120-A0.2-FR	1.96	11.26	11.53	11.75	11.83	22.96	23.02	23.30	23.54
302-N120-A0.4-FR	1.96	10.02	10.96	11.31	11.41	19.65	20.55	21.59	22.40
302-N120-A0.6-FR	1.96	9.21	10.72	11.23	11.38	16.00	17.90	19.77	21.15
302-N150-A0-FR	1.99	20.34	20.34	20.34	20.34	24.21	24.21	24.21	24.21
302-N150-A0.2-FR	1.99	18.99	19.07	19.27	19.49	22.94	23.07	23.36	23.61
302-N150-A0.4-FR	1.99	15.70	16.29	17.00	17.67	19.64	20.60	21.62	22.42
302-N150-A0.6-FR	1.99	12.18	14.13	15.74	17.05	16.11	18.87	20.72	21.77

Table 4 Web crippling strengths of austenitic stainless steel sections predicted from finite element analysis

A. a/h for centred circular web opening case

Specimen	Thickness	Unfastened FEA load per web, P_{FEA}					Fastened FEA load per web, P_{FEA}				
	t	$A(0)$	$A(0.2)$	$A(0.4)$	$A(0.6)$	$A(0.8)$	$A(0)$	$A(0.2)$	$A(0.4)$	$A(0.6)$	$A(0.8)$
	(mm)	(kN)	(kN)	(kN)	(kN)	(kN)	(kN)	(kN)	(kN)	(kN)	(kN)
142-N100-FR	1.27	5.77	5.48	5.16	4.87	-	8.80	6.36	6.02	5.72	-
142-N100-FR	4.00	61.23	57.26	52.80	48.75	-	83.33	71.90	66.49	61.48	-
142-N100-FR	6.00	140.84	132.75	120.98	109.68	-	202.76	163.27	150.41	138.26	-
142-N120-FR	1.27	6.26	5.96	5.65	5.36	5.06	7.81	6.68	6.32	6.00	5.65
142-N120-FR	4.00	66.17	61.85	57.08	52.68	48.56	80.42	77.73	71.82	66.24	60.67
142-N120-FR	6.00	152.62	143.70	131.34	119.77	108.61	183.39	177.81	163.89	150.28	135.23
142-N150-FR	1.28	6.44	6.11	5.79	5.49	5.18	9.78	7.37	7.00	6.65	6.29
142-N150-FR	4.00	70.82	66.21	61.46	56.98	52.62	95.99	87.14	80.95	75.20	69.24
142-N150-FR	6.00	165.72	155.96	143.86	132.18	120.74	217.75	199.94	185.99	172.48	157.67
202-N100-FR	1.39	5.78	5.51	5.13	4.76	-	9.74	6.70	6.29	5.91	-
202-N100-FR	4.00	54.47	50.86	46.35	42.29	-	103.99	68.49	63.26	58.31	-
202-N100-FR	6.00	128.51	121.13	108.95	97.98	-	187.46	158.11	145.94	133.13	-
202-N120-FR	1.39	6.04	5.74	5.35	4.96	-	11.11	7.49	7.02	6.58	-
202-N120-FR	4.00	57.52	53.48	48.74	44.36	-	91.41	73.23	67.41	62.09	-
202-N120-FR	6.00	137.43	128.37	115.65	103.57	-	204.00	171.37	157.44	143.65	-
202-N150-FR	1.39	6.48	6.13	4.94	4.54	-	11.67	8.03	7.53	7.05	-
202-N150-FR	4.00	62.15	57.70	51.74	47.14	-	96.38	80.37	73.82	67.86	-
202-N150-FR	6.00	188.24	139.30	124.60	112.12	-	219.28	189.77	174.20	159.38	-
302-N100-FR	1.98	11.19	10.73	9.87	9.11	-	19.24	13.35	13.81	11.12	-
302-N100-FR	4.00	50.17	47.18	42.95	39.52	-	81.17	68.90	61.61	51.08	-
302-N100-FR	6.00	118.91	112.14	99.83	89.92	-	183.10	143.38	132.13	120.61	-
302-N120-FR	1.98	11.46	10.98	10.10	9.27	-	19.86	14.24	12.84	11.94	-
302-N120-FR	4.00	52.00	48.67	44.18	40.43	-	86.32	63.50	58.11	52.77	
302-N120-FR	6.00	124.50	116.63	103.98	92.74	-	194.15	151.74	138.54	125.67	

A. Continued

Specimen	Thickness	Unfastened FEA load per web, P_{FEA}					Fastened FEA load per web, P_{FEA}				
	t	*A*(*0*)	*A*(*0.2*)	*A*(*0.4*)	*A*(*0.6*)	*A*(*0.8*)	*A*(*0*)	*A*(*0.2*)	*A*(*0.4*)	*A*(*0.6*)	*A*(*0.8*)
	(*mm*)	(*kN*)	(*kN*)	(*kN*)	(*kN*)	(*kN*)	(*kN*)	(*kN*)	(*kN*)	(*kN*)	(*kN*)
302-N150-FR	1.99	20.04	13.33	11.76	10.05	-	20.88	15.60	13.81	12.57	-
302-N150-FR	4.00	87.94	57.03	46.94	42.13	-	92.51	67.77	61.61	55.70	-
302-N150-FR	6.00	169.51	127.17	113.28	100.89	-	207.86	163.29	148.07	133.82	-

B. *a*/*h* for offset circular web opening case

Specimen	Thickness	Unfastened FEA load per web, P_{FEA}				Fastened FEA load per web, P_{FEA}			
	t	*A*(*0*)	*A*(*0.2*)	*A*(*0.4*)	*A*(*0.6*)	*A*(*0*)	*A*(*0.2*)	*A*(*0.4*)	*A*(*0.6*)
	(*mm*)	(*kN*)	(*kN*)	(*kN*)	(*kN*)	(*kN*)	(*kN*)	(*kN*)	(*kN*)
142-N100-FR	1.27	5.77	5.52	5.13	4.65	8.97	8.69	8.23	7.80
142-N100-FR	4.00	61.23	59.76	57.06	54.29	83.02	82.45	81.47	80.50
142-N100-FR	6.00	140.84	138.58	134.27	128.34	185.83	185.23	183.71	181.96
142-N120-FR	1.27	6.05	5.80	5.42	4.98	9.37	8.95	8.47	8.09
142-N120-FR	4.00	65.46	63.76	60.97	58.46	88.01	87.40	86.27	85.13
142-N120-FR	6.00	151.74	149.41	144.33	138.34	198.83	198.04	196.29	194.33
142-N150-FR	1.28	6.44	6.19	5.84	5.46	9.47	9.11	8.72	8.37
142-N150-FR	4.00	70.82	69.03	66.53	64.06	95.20	94.63	93.64	92.54
142-N150-FR	6.00	165.72	162.92	157.51	151.73	217.31	216.41	214.32	211.70
202-N100-FR	1.39	5.61	5.43	5.02	4.58	10.55	10.29	9.94	9.51
202-N100-FR	4.00	54.47	59.32	50.48	48.36	104.13	85.70	84.48	83.35
202-N100-FR	6.00	128.51	136.08	124.66	117.28	227.47	224.99	208.10	193.09
202-N120-FR	1.39	6.04	6.01	5.43	4.98	10.47	10.20	9.70	9.26
202-N120-FR	4.00	57.52	56.00	53.63	51.58	104.53	98.26	91.97	87.51
202-N120-FR	6.00	137.43	135.13	130.45	125.37	204.21	203.50	202.13	200.40
202-N150-FR	1.39	7.09	6.22	5.84	5.44	11.67	11.25	10.75	10.27
202-N150-FR	4.00	62.14	60.64	58.59	56.58	96.48	95.60	95.35	92.96
202-N150-FR	6.00	149.47	147.11	142.49	137.47	219.73	218.82	217.00	214.92
302-N100-FR	1.98	11.19	10.89	10.61	10.55	19.24	18.96	18.66	18.31
302-N100-FR	2.00	50.21	48.75	46.29	43.91	81.18	80.48	79.13	77.72
302-N100-FR	4.00	119.02	116.56	112.28	108.10	183.17	182.54	181.15	179.39
302-N120-FR	1.98	11.46	11.32	11.29	11.25	19.86	19.67	19.36	18.89
302-N120-FR	2.00	52.00	50.61	48.34	46.10	86.34	85.38	83.40	81.42
302-N120-FR	4.00	124.50	122.20	118.14	114.05	230.49	212.29	194.60	188.83
302-N150-FR	1.99	19.19	18.47	17.22	14.92	28.56	28.53	28.38	27.19
302-N150-FR	2.00	76.61	73.19	68.27	60.71	120.82	120.80	120.74	120.02
302-N150-FR	4.00	169.51	163.48	155.50	143.70	208.35	246.05	241.93	227.42

C. *x*/*h* for offset circular web opening case

Specimen	Thickness	Unfastened FEA load per web, $P_{(FEA)}$				Fastened FEA load per web, P_{FEA}			
	t	*X*(*0*)	*X*(*0.2*)	*X*(*0.4*)	*X*(*0.6*)	*X*(*0*)	*X*(*0.2*)	*X*(*0.4*)	*X*(*0.6*)
	(*mm*)	(*kN*)	(*kN*)	(*kN*)	(*kN*)	(*kN*)	(*kN*)	(*kN*)	(*kN*)
142-N100-A0-FR	1.27	5.67	5.67	5.67	5.67	8.80	8.80	8.80	8.80
142-N100-A0.2-FR	1.27	5.28	5.28	5.35	5.43	8.47	8.48	8.51	8.80
142-N100-A0.4-FR	1.27	4.81	4.81	4.91	5.05	7.63	7.87	8.05	8.21

C. Continued

Specimen	Thickness	Unfastened FEA load per web, $P_{(FEA)}$				Fastened FEA load per web, P_{FEA}			
	t	$X(0)$	$X(0.2)$	$X(0.4)$	$X(0.6)$	$X(0)$	$X(0.2)$	$X(0.4)$	$X(0.6)$
	(*mm*)	(*kN*)	(*kN*)	(*kN*)	(*kN*)	(*kN*)	(*kN*)	(*kN*)	(*kN*)
142-N100-A0.6-FR	1.27	4.23	4.30	4.40	4.60	6.65	7.08	7.42	7.71
142-N100-A0.8-FR	1.27	3.44	3.73	4.72	4.98	5.58	6.54	6.81	7.07
142-N120-A0-FR	1.27	5.96	5.96	5.96	5.96	9.31	9.31	9.31	9.31
142-N120-A0.2-FR	1.27	5.51	5.57	5.64	5.72	8.76	8.80	8.85	8.94
142-N120-A0.4-FR	1.27	5.01	5.10	5.21	5.35	7.81	8.04	8.27	8.46
142-N120-A0.6-FR	1.27	4.53	4.60	4.74	4.92	6.93	7.36	7.70	8.02
142-N120-A0.8-FR	1.27	3.79	4.13	4.40	4.66	5.89	6.56	7.13	7.66
142-N150-A0-FR	1.28	7.50	7.50	7.50	7.50	9.47	9.47	9.47	9.47
142-N150-A0.2-FR	1.28	5.90	5.97	6.06	6.14	8.85	8.89	8.96	9.05
142-N150-A0.4-FR	1.28	5.38	5.50	5.64	5.78	8.06	8.27	8.27	8.46
142-N150-A0.6-FR	1.28	4.88	5.07	5.24	5.42	7.24	7.65	8.00	8.32
142-N150-A0.8-FR	1.28	4.39	4.69	4.94	5.19	6.27	6.93	7.49	8.00
202-N100-A0-FR	1.39	5.73	5.73	5.73	5.73	12.48	12.48	12.48	12.48
202-N100-A0.2-FR	1.39	5.27	5.43	5.49	5.53	9.73	9.75	9.78	9.85
202-N100-A0.4-FR	1.39	4.68	4.90	5.03	5.16	8.72	9.01	9.28	9.52
202-N100-A0.6-FR	1.39	4.06	4.29	4.53	4.77	7.51	8.09	8.65	9.06
202-N120-A0-FR	1.39	5.97	5.97	5.97	5.97	10.65	10.65	10.65	10.65
202-N120-A0.2-FR	1.39	5.53	5.66	5.73	5.78	10.22	10.23	10.31	10.40
202-N120-A0.4-FR	1.39	4.95	5.14	5.27	5.41	9.01	9.29	9.60	9.85
202-N120-A0.6-FR	1.39	4.30	4.54	5.27	5.58	7.78	8.38	8.96	9.43
202-N150-A0-FR	1.45	7.81	7.81	7.81	7.81	12.28	12.28	12.28	12.28
202-N150-A0.2-FR	1.45	6.51	6.64	6.71	6.76	11.52	11.56	11.67	11.81
202-N150-A0.4-FR	1.45	5.82	6.05	6.21	6.36	10.25	10.59	10.96	11.27
202-N150-A0.6-FR	1.45	5.13	5.42	5.66	5.93	8.95	9.62	10.25	10.77
302-N100-A0-FR	1.98	11.21	11.21	11.21	11.21	18.81	18.81	18.81	18.81
302-N100-A0.2-FR	1.98	10.38	10.58	10.77	10.92	18.41	18.45	18.53	23.78
302-N120-A0-FR	1.96	11.25	11.25	11.25	11.25	19.50	19.50	19.50	19.50
302-N120-A0.2-FR	1.96	10.71	10.95	11.06	11.81	19.13	19.13	19.25	19.35
302-N120-A0.4-FR	1.96	9.83	10.64	10.98	11.07	17.50	18.10	18.68	19.04
302-N120-A0.6-FR	1.96	9.05	10.51	10.92	11.03	14.56	16.23	17.74	18.67
302-N150-A0-FR	1.99	20.08	20.08	20.08	20.08	23.37	23.37	23.37	23.37
302-N150-A0.2-FR	1.99	17.84	18.60	18.74	18.90	20.04	20.10	20.28	20.42
302-N150-A0.4-FR	1.99	14.87	15.84	16.49	17.25	17.72	18.51	19.31	19.89
302-N150-A0.6-FR	1.99	11.96	13.88	15.42	16.62	14.68	16.69	17.96	19.14

Table 5 Web crippling strengths of ferritic stainless steel sections predicted from finite element analysis

A. a/h for centred circular web opening case

Specimen	Thickness	Unfastened FEA load per web, P_{FEA}					Fastened FEA load per web, P_{FEA}				
	t	$A(0)$	$A(0.2)$	$A(0.4)$	$A(0.6)$	$A(0.8)$	$A(0)$	$A(0.2)$	$A(0.4)$	$A(0.6)$	$A(0.8)$
	(*mm*)	(*kN*)	(*kN*)	(*kN*)	(*kN*)	(*kN*)	(*kN*)	(*kN*)	(*kN*)	(*kN*)	(*kN*)
142-N100-FR	1.27	6.29	5.94	5.63	5.34	-	9.65	6.86	6.52	6.21	-
142-N100-FR	4.00	68.47	63.46	58.53	54.04	-	89.66	77.78	72.33	67.17	-
142-N100-FR	6.00	158.68	147.71	134.87	122.96	-	196.41	175.16	163.03	150.12	-
142-N120-FR	1.27	6.63	6.25	5.92	5.63	5.32	10.04	7.24	6.89	6.56	5.32

A. Continued

Specimen	Thickness	Unfastened FEA load per web, P_{FEA}					Fastened FEA load per web, P_{FEA}				
	t	*A*(*0*)	*A*(*0.2*)	*A*(*0.4*)	*A*(*0.6*)	*A*(*0.8*)	*A*(*0*)	*A*(*0.2*)	*A*(*0.4*)	*A*(*0.6*)	*A*(*0.8*)
	(*mm*)	(*kN*)	(*kN*)	(*kN*)	(*kN*)	(*kN*)	(*kN*)	(*kN*)	(*kN*)	(*kN*)	(*kN*)
142-N120-FR	4.00	73.08	67.80	62.48	57.70	53.40	96.60	84.51	78.63	73.02	67.79
142-N120-FR	6.00	171.18	158.23	145.05	132.80	121.11	215.85	193.65	180.08	166.47	151.42
142-N150-FR	1.28	7.05	6.66	6.30	5.97	5.65	10.55	8.00	7.62	7.26	6.87
142-N150-FR	4.00	79.39	73.71	68.18	62.97	58.12	105.19	95.06	88.56	82.53	76.47
142-N150-FR	6.00	186.43	173.16	159.60	146.73	121.11	240.71	219.56	205.00	191.06	175.58
202-N100-FR	1.39	6.08	5.79	5.42	5.04	-	10.65	7.12	6.71	6.32	-
202-N100-FR	4.00	60.14	55.84	50.76	46.55	-	89.14	72.18	67.20	62.21	-
202-N100-FR	6.00	144.68	134.31	120.74	109.10	-	188.82	167.17	156.07	144.02	-
202-N120-FR	1.39	6.34	6.02	5.63	5.24	-	12.01	7.98	7.51	7.07	-
202-N120-FR	4.00	81.44	60.94	55.47	50.46	-	96.89	77.58	72.39	66.51	-
202-N120-FR	6.00	153.98	142.23	128.10	115.25	-	212.73	182.58	169.04	155.93	-
202-N150-FR	1.39	6.78	6.42	5.11	4.69	-	12.44	8.57	8.07	7.60	-
202-N150-FR	4.00	84.01	65.44	59.63	54.23	-	104.76	85.83	79.19	73.12	-
202-N150-FR	6.00	167.27	154.54	137.92	124.11	-	236.88	204.52	188.58	173.90	-
302-N100-FR	1.98	11.53	11.01	10.15	9.34	-	20.83	14.09	13.81	11.48	-
302-N100-FR	4.00	54.00	50.53	46.15	42.56	-	84.47	64.71	61.61	54.73	-
302-N100-FR	6.00	130.86	121.77	108.76	98.41	-	186.57	153.13	141.44	129.78	-
302-N120-FR	1.98	11.77	11.21	10.34	9.48	-	21.70	15.09	13.43	12.38	-
302-N120-FR	4.00	55.54	51.86	47.42	42.32	-	92.09	67.33	61.92	56.56	-
302-N120-FR	6.00	136.34	126.52	112.74	101.40	-	202.45	161.84	148.40	135.54	-
302-N150-FR	1.99	19.76	13.41	11.82	10.08	-	22.42	16.33	14.25	12.99	-
302-N150-FR	4.00	83.39	55.52	49.81	49.81	-	100.34	71.79	65.75	55.70	-
302-N150-FR	6.00	189.16	137.53	122.36	109.15	-	224.90	174.86	159.39	144.90	-

B. *a*/*h* for offset circular web opening case

Specimen	Thickness	Unfastened FEA load per web, P_{FEA}				Fastened FEA load per web, P_{FEA}			
	t	*A*(*0*)	*A*(*0.2*)	*A*(*0.4*)	*A*(*0.6*)	*A*(*0*)	*A*(*0.2*)	*A*(*0.4*)	*A*(*0.6*)
	(*mm*)	(*kN*)	(*kN*)	(*kN*)	(*kN*)	(*kN*)	(*kN*)	(*kN*)	(*kN*)
142-N100-FR	1.27	6.29	6.01	5.59	5.09	9.65	9.64	9.12	8.57
142-N100-FR	4.00	68.47	66.67	63.62	61.01	89.66	89.46	88.62	87.82
142-N100-FR	6.00	158.68	156.37	151.25	145.19	196.41	196.30	195.51	194.78
142-N120-FR	1.27	6.63	6.33	5.94	5.45	10.04	9.95	9.35	8.83
142-N120-FR	4.00	73.08	71.15	68.39	65.83	96.73	96.19	95.14	94.14
142-N120-FR	6.00	171.18	168.40	162.79	156.64	215.85	215.67	214.46	213.13
142-N150-FR	1.28	7.05	6.78	6.45	6.00	10.55	10.11	9.57	9.12
142-N150-FR	4.00	79.39	77.43	74.92	72.38	105.78	105.23	104.16	102.96
142-N150-FR	6.00	186.43	183.69	178.28	172.20	240.71	240.46	238.88	236.66
202-N100-FR	1.39	6.08	5.80	5.37	4.95	11.23	10.65	10.63	9.89
202-N100-FR	4.00	60.14	58.47	55.65	53.19	89.14	88.78	88.49	87.89
202-N100-FR	6.00	144.68	141.92	136.74	131.35	194.25	193.77	193.61	192.96
202-N120-FR	1.39	6.34	6.04	5.62	5.19	12.01	10.91	10.22	9.63
202-N120-FR	4.00	81.44	61.88	59.20	56.78	96.89	96.88	95.59	93.83
202-N120-FR	6.00	153.98	151.23	145.88	140.47	212.73	212.56	212.11	211.22
202-N150-FR	1.39	6.78	6.46	6.06	5.65	12.44	11.95	11.27	10.74

B. Continued

Specimen	Thickness	Unfastened FEA load per web, P_{FEA}				Fastened FEA load per web, P_{FEA}			
	t	$A(0)$	$A(0.2)$	$A(0.4)$	$A(0.6)$	$A(0)$	$A(0.2)$	$A(0.4)$	$A(0.6)$
	(*mm*)	(*kN*)	(*kN*)	(*kN*)	(*kN*)	(*kN*)	(*kN*)	(*kN*)	(*kN*)
202-N150-FR	4.00	84.01	67.11	64.53	62.22	104.76	103.70	101.89	100.40
202-N150-FR	6.00	187.98	164.55	164.53	154.11	236.88	236.41	234.72	232.81
302-N100-FR	1.98	11.53	11.26	10.73	10.66	20.83	20.57	20.18	19.39
302-N100-FR	2.00	54.00	51.90	48.72	45.98	84.47	84.23	83.48	82.37
302-N100-FR	4.00	130.86	127.70	122.54	117.63	186.57	186.52	185.58	184.58
302-N120-FR	1.98	11.77	11.44	11.39	11.34	21.70	21.39	20.49	19.64
302-N120-FR	2.00	55.54	53.52	50.76	48.09	92.09	91.57	89.54	86.73
302-N120-FR	4.00	136.34	133.38	128.65	123.83	202.45	202.29	201.40	199.77
302-N150-FR	1.99	19.76	18.97	17.26	15.01	22.42	21.75	20.87	21.44
302-N150-FR	2.00	83.39	79.20	73.11	64.44	100.34	97.99	93.43	87.77
302-N150-FR	4.00	189.16	180.86	169.93	154.54	224.90	223.78	219.78	211.63

C. x/h for offset circular web opening case

Specimen	Thickness	Unfastened FEA load per web, $P_{(FEA)}$				Fastened FEA load per web, P_{FEA}			
	t	$X(0)$	$X(0.2)$	$X(0.4)$	$X(0.6)$	$X(0)$	$X(0.2)$	$X(0.4)$	$X(0.6)$
	(*mm*)	(*kN*)	(*kN*)	(*kN*)	(*kN*)	(*kN*)	(*kN*)	(*kN*)	(*kN*)
142-N100-A0-FR	1.27	6.18	6.18	6.18	6.18	9.74	9.74	9.74	9.74
142-N100-A0.2-FR	1.27	5.68	5.79	5.89	5.96	9.37	9.36	9.42	9.74
142-N100-A0.4-FR	1.27	5.13	5.27	5.44	5.59	8.41	8.64	8.85	9.74
142-N100-A0.6-FR	1.27	4.55	4.70	4.88	5.09	7.25	7.77	8.16	9.74
142-N100-A0.8-FR	1.27	3.73	3.97	4.27	4.54	6.08	7.08	7.36	7.65
142-N120-A0-FR	1.27	6.49	6.49	6.49	6.49	10.27	10.27	10.27	10.27
142-N120-A0.2-FR	1.27	6.01	6.13	6.23	6.29	9.69	9.72	9.79	9.88
142-N120-A0.4-FR	1.27	5.43	5.60	5.78	5.92	8.64	8.90	9.10	9.32
142-N120-A0.6-FR	1.27	4.88	5.03	5.24	5.43	7.52	7.99	8.39	8.75
142-N120-A0.8-FR	1.27	4.09	4.39	4.65	4.90	6.43	7.15	7.76	8.30
142-N150-A0-FR	1.28	6.95	6.95	6.95	6.95	10.50	10.50	10.50	10.50
142-N150-A0.2-FR	1.28	6.48	6.62	6.70	6.75	9.84	9.90	9.97	10.07
142-N150-A0.4-FR	1.28	5.88	6.10	6.28	6.40	8.84	9.08	9.29	9.50
142-N150-A0.6-FR	1.28	5.32	5.56	5.78	5.96	7.90	8.34	8.73	9.06
142-N150-A0.8-FR	1.28	4.73	5.01	5.24	5.47	6.91	7.60	8.19	8.69
202-N100-A0-FR	1.39	6.07	6.07	6.07	6.07	10.97	10.97	10.97	10.97
202-N100-A0.2-FR	1.39	5.82	5.73	5.78	5.82	10.59	10.58	10.67	10.76
202-N100-A0.4-FR	1.39	5.42	5.13	5.28	5.42	9.29	9.57	9.91	10.22
202-N100-A0.6-FR	1.39	4.99	4.52	4.77	4.99	7.84	8.38	8.96	9.52
202-N120-A0-FR	1.39	6.31	6.31	6.31	6.31	11.52	11.52	11.52	11.52
202-N120-A0.2-FR	1.39	6.06	5.98	6.01	6.06	10.92	10.93	11.04	11.15
202-N120-A0.4-FR	1.39	5.66	5.38	5.52	5.66	9.51	9.80	10.13	10.47
202-N120-A0.6-FR	1.39	4.65	4.65	5.02	5.25	8.15	8.74	9.34	9.82
202-N150-A0-FR	1.45	7.39	7.39	7.39	7.39	13.08	13.08	13.08	13.08
202-N150-A0.2-FR	1.45	6.90	7.12	7.05	7.12	12.27	12.32	12.45	12.59
202-N150-A0.4-FR	1.45	6.16	6.36	6.52	6.68	10.78	11.12	11.50	11.83
202-N150-A0.6-FR	1.45	5.42	5.71	5.97	6.25	9.41	10.10	10.75	11.28
302-N100-A0-FR	1.98	11.55	11.55	11.55	11.55	20.15	20.15	20.15	20.15

C. Continued

Specimen	Thickness	Unfastened FEA load per web, $P_{(FEA)}$				Fastened FEA load per web, P_{FEA}			
	t	*X(0)*	*X(0.2)*	*X(0.4)*	*X(0.6)*	*X(0)*	*X(0.2)*	*X(0.4)*	*X(0.6)*
	(*mm*)	(*kN*)	(*kN*)	(*kN*)	(*kN*)	(*kN*)	(*kN*)	(*kN*)	(*kN*)
302-N100-A0.2-FR	1.98	10.62	10.89	11.13	11.28	19.83	19.82	19.93	20.01
302-N120-A0-FR	1.96	11.51	11.51	11.51	11.51	21.22	21.22	21.22	21.22
302-N120-A0.2-FR	1.96	11.07	11.07	11.19	11.24	20.72	20.74	20.91	21.03
302-N120-A0.4-FR	1.96	9.86	10.74	11.10	11.20	18.14	18.84	19.68	20.28
302-N120-A0.6-FR	1.96	10.51	10.51	11.03	11.16	14.99	16.63	18.27	19.49
302-N150-A0-FR	1.99	19.70	19.70	19.70	19.70	22.23	22.23	22.23	22.23
302-N150-A0.2-FR	1.99	18.47	18.47	18.68	18.90	21.03	21.12	21.36	21.61
302-N150-A0.4-FR	1.99	15.13	15.77	16.51	17.29	18.29	19.11	20.03	20.73
302-N150-A0.6-FR	1.99	11.93	13.92	15.50	16.73	15.28	17.70	18.97	19.74

and the 1.3 mm thick sections have the smallest reduction in strength or the highest strength reduction factor of almost unity.

Fig. 7(c) shows the ratio of the circular web opening location to the flat portion of the web (x/h) versus the strength reduction factor, for the three stainless steel grades. As can be seen, the reduction in strength is sensitive to the horizontal distance of the web openings to the bearing plates. As the ratio of x/h decreases from 0.6 to 0.2, the strength reduction factor decreases by 10%. Also, it can again be seen that austenitic grade has lower strength reduction factor compared to that of the other two stainless steel grades.

5. Reduction factor comparison with Uzzaman *et al*. (2012a, c)

For ease of reference, the reduction factor equations for the calculated solid web shear strength proposed by Uzzaman *et al*. (2012a, c) are summarised below:

For centered web opening

Free case

$$R_P = 1.05 - 0.54(\frac{a}{h}) + 0.01(\frac{N}{h}) \le 1 \quad (1)$$

Fixed case

$$R_P = 1.01 - 0.51(\frac{a}{h}) + 0.06(\frac{N}{h}) \le 1 \quad (2)$$

For offset web opening

Free case

$$R_P = 1.04 - 0.68(\frac{a}{h}) + 0.023(\frac{x}{h}) \le 1 \quad (3)$$

Fixed case

$$R_P = 1.00 - 0.45(\frac{a}{h}) + 0.09(\frac{x}{h}) \le 1 \quad (4)$$

where the limits for the reduction factor in Eqs. (1)-(4) are $h/t \le 156$, $N/t \le 84$, $N/h \le 0.63$, $a/h \le 0.8$, and $\theta = 90°$.

In order to evaluate the applicability of the proposed equations to cold-formed stainless steel grades, an extensive statistical analysis was performed on all four proposed equations. Table 6 compares the reduction factors determined from the finite element models to Eqs. (1)-(4) for cases of centred and offset web opening where the flange is unfastened to the bearing plate.

As can be seen from Table 6, the four equations proposed by Uzzaman *et al*. (2012a, c) for carbon steel are unconservative for the stainless steel grades, especially for the duplex stainless steel grade which are unconservative by up to 17%. As an example, for the duplex stainless steel grade, for the centred web opening case, the mean value of the web crippling reduction factors are 0.92 and 0.83 for the cases of flange unfastened and fastened to the bearing plate, respectively; the corresponding values of COV are 0.09 and 0.16, respectively. Similar values are reported for the case of the ferritic stainless steel grade. In the next section, new equations of reduction factors are proposed for each of the three stainless steel grades.

6. Proposed strength reduction factors

Tables 3 to 5 show the dimensions considered and web crippling strengths of the duplex, austenitic and ferritic stainless steel sections predicted from the finite element analysis. Using bivariate linear regression analysis, two unified strength reduction factor equations (R_p) on the solid web shear strength for three stainless steel grades with web openings are proposed. The equations are as follows:

Centred web opening

$$R_p = \alpha - \gamma(\frac{a}{h}) + \lambda(\frac{N}{h}) \le 1 \quad (5)$$

Offset web opening

$$R_p = \rho - \mu\left(\frac{a}{h}\right) + \zeta\left(\frac{x}{h}\right) \le 1 \quad (6)$$

Table 6 Comparison of web crippling strength reduction factor for cold-formed stainless steel lipped channel-sections with reduction factors equations proposed by Uzzaman *et al*. (2012a, c)

A. Flange unfastened to the bearing plate

Specimen	Factored resistance (Eq. (1))	Factored resistance (Eq. (3))	Reduction factor						Comparison with resistance from Uzzaman *et al*. (2012a, c) R/R_{Lian}					
			Duplex		Ferritic		Austenitic							
			$R = P(Opening)/P(A0)$		$R = P(Opening)/P(A0)$		$R=P(Opening)/P(A0)$		Duplex		Ferritic		Austenitic	
	Centred	Offset	Centred	Offset	Centred	Offset	Centred	Offset	Centred	Offset	Centred	Offset	Centred	Offset
202-N100-MA0	1.06	1.05	1.00	1.00	1.00	1.00	1.00	1.00	0.95	0.95	0.95	0.96	0.95	0.95
202-N100-MA0.2	1.00	0.99	0.95	0.98	0.95	0.95	0.95	0.97	0.95	0.99	0.95	0.98	0.95	0.98
202-N120-MA0	1.06	1.05	1.00	1.00	1.00	1.00	1.00	1.00	0.95	0.95	0.95	0.96	0.95	0.95
202-N120-MA0.2	1.00	0.99	0.95	0.98	0.95	0.95	0.95	1.00	0.95	0.99	0.95	0.98	0.95	1.01
202-N150-MA0	1.06	1.06	1.00	1.00	1.00	1.00	1.00	1.00	0.95	0.95	0.95	0.96	0.95	0.95
202-N150-MA0.2	1.00	0.99	0.94	0.98	0.95	0.95	0.95	0.88	0.93	0.99	0.94	0.98	0.94	0.90
302-N100-MA0	1.05	1.05	1.00	1.00	1.00	1.00	1.00	1.00	0.95	0.95	0.95	0.96	0.95	0.95
302-N120-MA0	1.05	1.05	1.00	1.00	1.00	1.00	1.00	1.00	0.95	0.95	0.95	0.96	0.95	0.95
302-N120-MA0.2	1.00	0.99	0.95	0.99	0.95	0.97	0.96	0.99	0.95	1.01	0.95	1.00	0.96	1.00
302-N150-MA0	1.06	1.05	1.00	1.00	1.00	1.00	1.00	1.00	0.95	0.95	0.95	0.96	0.95	0.96
302-N150-MA0.2	1.00	0.98	0.67	0.99	0.68	0.96	0.66	0.96	0.67	1.00	0.68	0.99	0.66	0.99
Mean, *Pm*									0.92	1.00	0.92	0.97	0.92	0.96
Coefficient of variation, *Vp*									0.09	0.05	0.09	0.01	0.09	0.03

B. Flange fastened to the bearing plate

Specimen	Factored resistance from Lian (Eq. (2))	Factored resistance from Lian (Eq. (4))	Reduction factor						Comparison with resistance from Uzzaman *et al.* (2012a, c) R/R_{Lian}					
			Duplex		Ferritic		Austenitic							
			$R = P(Hole)/P(A0)$		$R = P(Hole)/P(A0)$		$R = P(Hole)/P(A0)$		Duplex		Ferritic		Austenitic	
	Centred	Offset	Centred	Offset	Centred	Offset	Centred	Offset	Centred	Offset	Centred	Offset	Centred	Offset
202-N100-MA0	1.04	1.00	1.00	1.00	1.00	1.00	1.00	1.00	0.96	0.96	0.96	1.00	0.96	1.00
202-N100-MA0.2	0.99	0.95	0.65	0.96	0.67	0.95	0.69	0.98	0.66	0.96	0.68	0.97	0.69	1.00
202-N120-MA0	1.05	1.00	1.00	1.00	1.00	1.00	1.00	1.00	0.96	0.95	0.96	1.00	0.96	1.00
202-N120-MA0.2	1.00	0.95	0.66	0.96	0.66	0.91	0.67	0.97	0.67	0.95	0.67	0.93	0.68	1.00
202-N150-MA0	1.06	1.00	1.00	1.00	1.00	1.00	1.00	1.00	0.95	1.00	0.95	1.00	0.95	1.00
202-N150-MA0.2	1.00	0.95	0.70	0.96	0.69	0.96	0.69	0.96	0.70	0.99	0.69	0.99	0.69	0.99
302-N100-MA0	1.03	1.00	1.00	1.00	1.00	1.00	1.00	1.00	0.97	0.97	0.97	1.00	0.97	1.00
302-N120-MA0	1.03	1.00	1.00	1.00	1.00	1.00	1.00	1.00	0.97	0.97	0.97	1.00	0.97	1.00
302-N120-MA0.2	0.98	0.96	0.65	1.00	0.70	0.99	0.72	0.99	0.67	1.01	0.71	1.01	0.73	1.02
302-N150-MA0	1.04	1.00	1.00	1.00	1.00	1.00	1.00	1.00	0.96	1.00	0.96	1.00	0.96	1.00
302-N150-MA0.2	0.99	0.96	0.70	1.00	0.73	0.97	0.75	1.00	0.71	1.03	0.74	1.00	0.76	1.03
Mean, *Pm*									0.83	0.98	0.85	0.99	0.85	1.00
Coefficient of variation, *Vp*									0.18	0.03	0.16	0.02	0.16	0.01

Table 7 Coefficients of the proposed strength reduction factor equations

	Stainless steel grade	Coefficient	Unfastened to bearing plate	Fastened to bearing plate
Strength reduction factor Eqs. (5-6)	EN 1.4462 (Duplex)	α	0.93	0.61
		γ	0.31	0.26
		λ	0.04	0.33
		ρ	0.94	0.87
		μ	0.25	0.32
		ζ	0.06	0.20
	EN 1.4404 (Austenitic)	α	0.91	0.75
		γ	0.35	0.33
		λ	0.08	0.22
		ρ	0.88	0.88
		μ	0.26	0.30
		ζ	0.20	0.21
	EN 1.4003 (Ferritic)	α	0.87	0.86
		γ	0.35	0.37
		λ	0.12	0.17
		ρ	0.91	0.85
		μ	0.17	0.33
		ζ	0.16	0.21

Table 8 Statistical analysis of strength reduction factor

A. Duplex stainless steel grade

Statistical parameters	Centred circular web opening $R_{(FEA)} / R_p$		Offset circular web opening $R_{(FEA)} / R_p$	
	Unfastened to bearing plate	Fastened to bearing plate	Unfastened to bearing plate	Fastened to bearing plate
Number of data	81	87	84	81
Mean, P_m	1.00	1.00	1.00	1.00
Coefficient of variation, V_p	0.06	0.10	0.05	0.04
Reliability index, β	2.76	2.62	2.78	2.80
Resistance factor, ϕ	0.85	0.85	0.85	0.85

The limits for the reduction factor Eqs. (5)-(6) are $h/t \leq 157.68$, $N/t \leq 120.97$, $N/h \leq 1.15$, $a/h \leq 0.8$, and $\theta = 90°$.

The coefficients α, γ, λ, ρ, μ and ζ of the equations are calibrated with the stainless steel analysis results, and the coefficients are presented in Table 7.

7. Comparison of numerical results with proposed reduction factors

For the three stainless steels grades, the values of the strength reduction factor (R) obtained from the numerical results are compared with the values of the proposed strength reduction factor (R_p) calculated using Eqs. (5) and (6). The results for C142, C202 and C302 are shown in Figs. 8, 9 and 10. In order to evaluate the accuracy and reliability of the proposed equations, extensive statistical reliability analyses are performed. The results are summarized in Table 8. It should be noted, in calculating the reliability index, the resistance factor of $\phi = 0.85$ was used, corresponding to the reliability index β from the NAS specification. According to the NAS specification, design rules are reliable if the reliability index is more than 2.5. As can be seen in Table 8, the proposed reduction factors are a good match with the numerical results for the both cases of flanges unfastened and flanges fastened to the bearing plates and particularly for the duplex stainless steel grade.

For example, for the centred circular web opening, the mean value of the web crippling reduction factor ratios are 1.00 and 1.00 for the cases of flange unfastened and flange fastened to the bearing plate, respectively. The corresponding values of COV are 0.06 and 0.10, respectively. Similarly,

Table 8 Continued

B. Austenitic stainless steel grade

Statistical parameters	Centred circular web opening $R_{(FEA)} / R_p$		Offset circular web opening $R_{(FEA)} / R_p$	
	Unfastened to bearing plate	Fastened to bearing plate	Unfastened to bearing plate	Fastened to bearing plate
Number of data	81	87	84	81
Mean, P_m	1.00	1.00	1.00	1.00
Coefficient of variation, V_p	0.06	0.10	0.05	0.04
Reliability index, β	2.76	2.62	2.78	2.80
Resistance factor, ϕ	0.85	0.85	0.85	0.85

C. Ferritic stainless steel grade

Statistical parameters	Centred circular web opening $R_{(FEA)} / R_p$		Offset circular web opening $R_{(FEA)} / R_p$	
	Unfastened to bearing plate	Fastened to bearing plate	Unfastened to bearing plate	Fastened to bearing plate
Number of data	86	87	84	81
Mean, P_m	1.00	1.00	1.00	1.00
Coefficient of variation, V_p	0.10	0.13	0.05	0.03
Reliability index, β	2.62	2.51	2.78	2.83
Resistance factor, ϕ	0.85	0.85	0.85	0.85

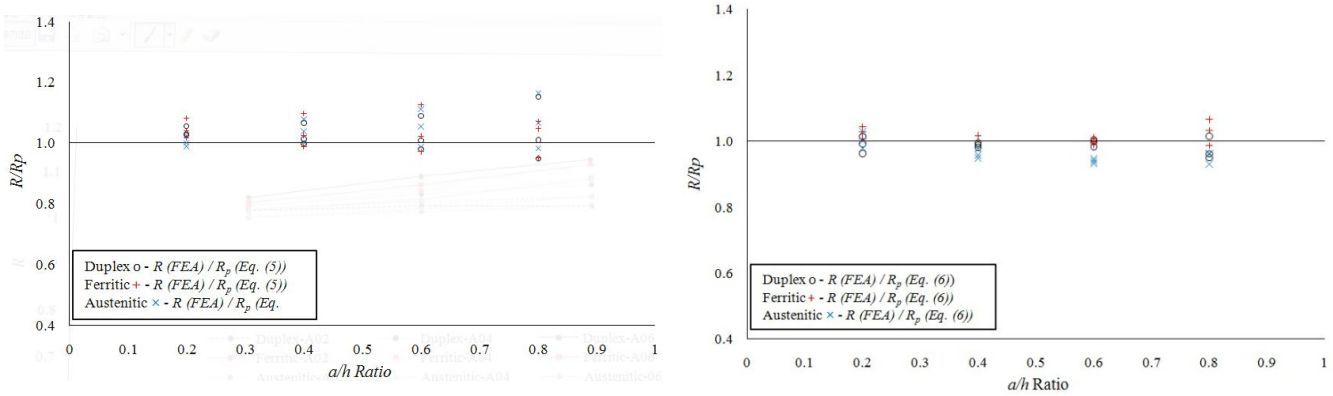

(a) With centered circular web opening (b) With offset circular web opening

Fig. 8 Comparison of strength reduction factor for C142 section for the case of flange unfastened to bearing plate

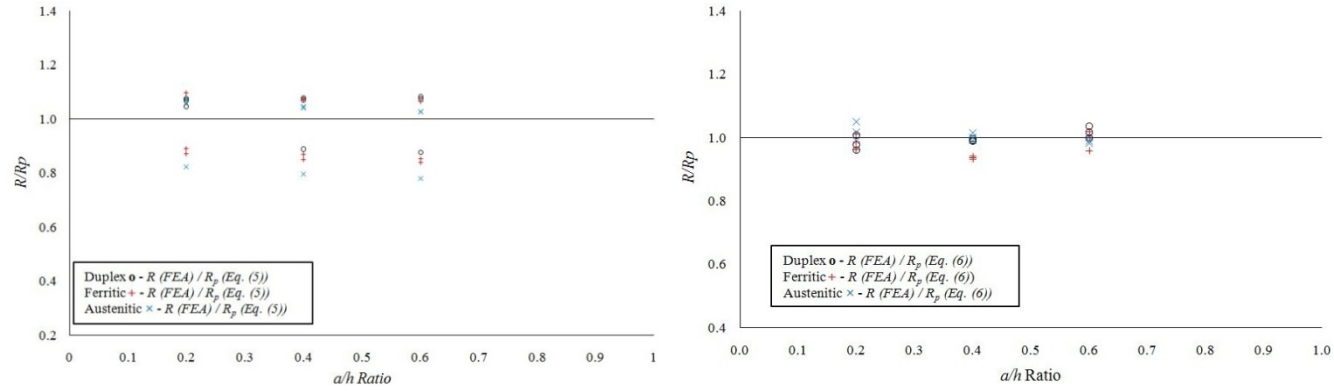

(a) With centered circular web opening (b) With offset circular web opening

Fig. 9 Comparison of strength reduction factor for C202 section for the case of flange unfastened to bearing plate

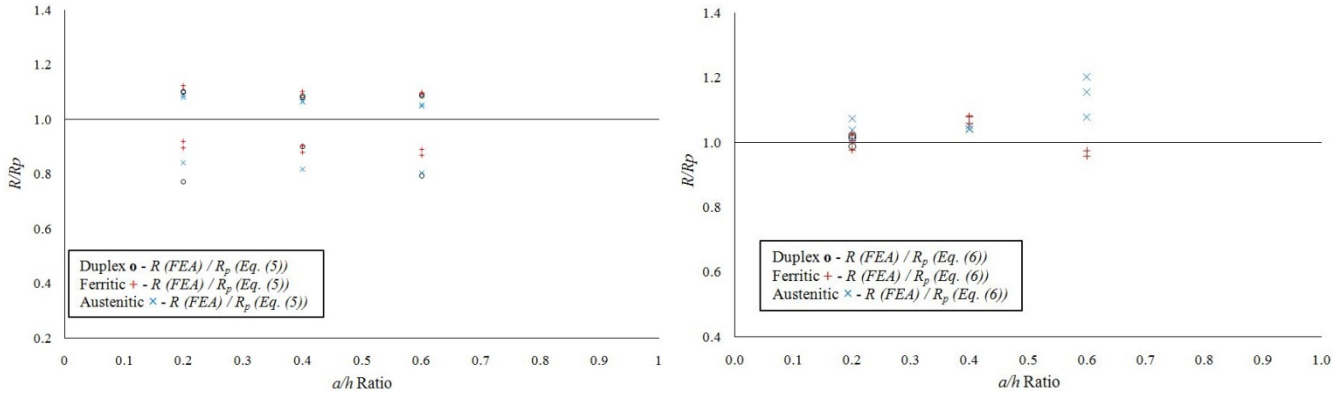

(a) With centered circular web opening (b) With offset circular web opening

Fig. 10 Comparison of strength reduction factor for C302 section for the case of flange unfastened to bearing plate

the reliability index values (β) are 2.76 and 2.62, respectively. For the offset circular web opening, the mean value of the web crippling reduction factor ratios are 1.00 and 1.00 for the cases of flange unfastened and flange fastened to the bearing plate, respectively. The corresponding values of COV are 0.05 and 0.04, respectively. Similarly, the reliability index values (β) are 2.78 and 2.80, respectively. Therefore, the proposed strength reduction factor equations are able to reliably predict the influence of the circular web openings on the web crippling strengths of cold-formed stainless steel lipped channel-sections under the Interior-two-flange (ITF) loading condition.

8. Conclusions

In this paper, an investigation into the effect of circular web openings on the web crippling strength of cold-formed

stainless steel lipped channel-sections has been conducted. For this purpose, a parametric study comprising 2,220 lipped channel-sections with various dimensions, thicknesses were considered for the three stainless steel grades, namely the duplex EN1.4462, austenitic EN1.4404 and ferretic EN1.4003. Cases with and without circular web openings under the interior-two-flange (ITF) loading condition were considered with web openings located centred and offset to the bearing plates.

In order to take into account the influence of the circular web openings, strength reduction factor equations were determined. The results obtained from the strength reduction factor equations were then compared to the results obtained from the equations proposed by Uzzaman *et al*. (2012a, c) for cold-formed carbon steel. It was observed that the predictions calculated from the strength reduction factor equations proposed for cold-formed carbon steel are unconservative for the stainless steel grades by up to 17%.

Based on the finite element results, new coefficients for web crippling strength reduction factor equations considering different web opening diameter and location in the web are proposed for both cases of flanges unfastened and flanges fastened to the bearing plates under the interior-two-flange (ITF) loading condition. Reliability analysis was performed in order to evaluate the reliability of the proposed strength reduction factors. It was demonstrated that the proposed strength reduction factors are generally conservative and agree well with the finite element results. The proposed new unified strength reduction factors are generally capable to produce reliable and safe design values when calibrated according to the NAS specification for resistance factor of 0.85 (φ = 0.85) for the interior-two-flange (ITF) loading condition.

References

ABAQUS (2014), Analysis User's Manual-Version 6.14-2; ABAQUS Inc., USA.

Arrayago, I., Real, E. and Gardner, L. (2015), "Description of stress–strain curves for stainless steel alloys", *Mater. Des.*, **87**, 540-552.

AS/NZS 4600 (2005), Cold-formed steel structures: AS/NZS 4600:2005, Standards Australia, Sydney, Australia.

ASCE 8-02 (2002), Specification for the Design of Cold-Formed Stainless Steel Structural Members: SEI/ASCE 8-02, Reston, VA, USA.

BS 5950-5 (1998), Structural use of steelwork in buildings, Part 5 Code of practice for the design of cold-formed sections. British Standards Institution, London, UK.

Chen, J. and Young, B. (2006), "Stress–strain curves for stainless steel at elevated temperatures", *Eng. Struct.*, **28**(2), 229-239.

Chen, Y., Chen, X. and Wang, C. (2015), "Experimental and finite element analysis research on cold-formed steel lipped channel beams under web crippling", *Thin-Wall. Struct.*, **87**, 41-52.

Dai, X. and Lam, D. (2010), "Axial compressive behaviour of stub concrete-filled columns with elliptical stainless steel hollow sections", *Steel Compos. Struct., Int. J.*, **10**(6), 517-539.

Eurocode-3 (2006), Design of steel structures: Part 1.3: General rules — Supplementary rules for cold-formed thin gauge members and sheeting; ENV 1993-1-3, European Committee for Standardization, Brussels, Belgium.

Gunalan, S. and Mahendran, M. (2015), "Web crippling tests of cold-formed steel channels under two flange load cases", *J. Constr. Steel Res.*, **110**, 1-15.

Keerthan, P. and Mahendran, M. (2012), "Shear behaviour and strength of LiteSteel beams with web openings", *Adv. Struct. Eng.*, **15**(2), 171-184.

Keerthan, P., Mahendran, M. and Steau, E. (2014), "Experimental study of web crippling behaviour of hollow flange channel beams under two flange load cases", *Thin-Wall. Struct.*, **85**, 207-219.

Kiymaz, G. and Seckin, E. (2014), "Behavior and design of stainless steel tubular member welded end connections", *Steel Compos. Struct., Int. J.*, **17**(3), 253-269.

Korvink, S.A., van den Berg, G.J. and van der Merwe, P. (1995), "Web crippling of stainless steel cold-formed beams", *J. Constr. Steel Res.*, **34**(2-3), 225-248.

Lawson, R.M., Basta, A. and Uzzaman, A. (2015), "Design of stainless steel sections with circular openings in shear", *J. Constr. Steel Res.*, **112**, 228-241.

Lian, Y., Uzzaman, A., Lim, J.B.P., Abdelal, G., Nash, D. and Young, B. (2016a), "Effect of web holes on web crippling strength of cold-formed steel channel sections under end-one-flange loading condition – Part I: Tests and finite element analysis", *Thin-Wall. Struct.*, **107**, 443-452.

Lian, Y., Uzzaman, A., Lim, J.B.P., Abdelal, G., Nash, D. and Young, B. (2016b), "Effect of web holes on web crippling strength of cold-formed steel channel sections under end-one-flange loading condition – Part II: Parametric study and proposed design equations", *Thin-Wall. Struct.*, **107**, 489-501. DOI: 10.1016/j.tws.2016.06.026

Lian, Y., Uzzaman, A., Lim, J.B.P., Abdelal, G., Nash, D. and Young, B. (2017a), "Web crippling behaviour of cold-formed steel channel sections with web holes subjected to interior-one-flange loading condition – Part I: Experimental and numerical investigation", *Thin-Wall. Struct.*, **111**, 103-112.

Lian, Y., Uzzaman, A., Lim, J.B.P., Abdelal, G., Nash, D. and Young, B. (2017b), "Web crippling behaviour of cold-formed steel channel sections with web holes subjected to interior-one-flange loading condition – Part II: Parametric study and proposed design equations", *Thin-Wall. Struct.*

NAS (2007), North American Specification for the Design of Cold-Formed Steel Structural Members; American Iron and Steel Institute, AISI S100-2007, AISI Standard.

Natário, P., Silvestre, N. and Camotim, D. (2014), "Web crippling failure using quasi-static FE models", *Thin-Wall. Struct.*, **84**, 34-49.

Rezvani, F.H., Yousefi, A.M. and Ronagh, H.R. (2015), "Effect of span length on progressive collapse behaviour of steel moment resisting frames", *Structures*, **3**, 81-89.

Rossi, B., Jaspart, J.P. and Rasmussen, K.J. (2009), "Combined distortional and overall flexural-torsional buckling of cold-formed stainless steel sections: Design", *J. Struct. Eng.*, **136**(4), 361-369.

Uzzaman, A., Lim, J.B.P., Nash, D., Rhodes, J. and Young, B. (2012a), "Web crippling behaviour of cold-formed steel channel sections with offset web holes subjected to interior-two-flange loading", *Thin-Wall. Struct.*, **50**(1), 76-86.

Uzzaman, A., Lim, J.B.P., Nash, D., Rhodes, J. and Young, B. (2012b), "Cold-formed steel sections with web openings subjected to web crippling under two-flange loading conditions – Part I: Tests and finite element analysis", *Thin-Wall. Struct.*, **56**, 38-48.

Uzzaman, A., Lim, J.B.P., Nash, D., Rhodes, J. and Young, B. (2012c), "Cold-formed steel sections with web openings subjected to web crippling under two-flange loading conditions – part II: Parametric study and proposed design equations",

Thin-Wall. Struct., **56**, 79-87.
Uzzaman, A., Lim, J.B.P., Nash, D., Rhodes, J. and Young, B. (2013), "Effect of offset web holes on web crippling strength of cold-formed steel channel sections under end-two-flange loading condition", *Thin-Wall. Struct*., **65**, 34-48.
Yousefi, A.M., Hosseini, M. and Fanaie, N. (2014), "Vulnerability assessment of progressive collapse of steel moment resistant frames", *Trends Appl. Sci. Res*., **9**(8), 450-460.
Yousefi, A.M., Lim, J.B.P., Asraf Uzzaman, Ying Lian, G. Charles Clifton, Young, B. (2016a), "Web crippling strength of cold-formed stainless steel lipped channel-sections with web openings subjected to Interior-One-Flange loading condition", S*teel and Composite Structures*, 21(3), 629-659.
Yousefi, A.M., Lim, J.B.P., Uzzaman, A., Lian, Y., Clifton, G.C. and Young, B. (2016b), "Design of cold-formed stainless steel lipped channel-sections with web openings subjected to web crippling under end-one-flange loading condition", *Adv. Struct. Eng*., DOI: 10.1177/1369433216670170
Yousefi, A.M., Lim, J.B.P., Uzzaman, A., Lian, Y., Clifton, G.C. and Young, B. (2016c), "Web crippling strength of cold-formed duplex stainless steel lipped channel-sections with web openings subjected to interior-one-flange loading condition", *Proceeding of The Wei-Wen Yu International Specialty Conference on Cold-Formed Steel Structures*, Baltimore, MD, USA, November.
Yousefi, A.M., Lim, J.B.P., Uzzaman, A., Lian, Y., Clifton, G.C. and Young, B. (2016d), "Web crippling design of cold-formed duplex stainless steel lipped channel-sections with web openings under end-one-flange loading condition", *Proceeding of The 11th Pacific Structural Steel Conference*, Shanghai, China, October.
Yousefi, A.M., Lim, J.B.P., Uzzaman, A., Clifton, G.C. and Young, B. (2016e), "Numerical study of web crippling strength in cold-formed austenitic stainless steel lipped channels with web openings subjected to interior-two-flange loading", *Proceeding of The 11th Pacific Structural Steel Conference*, Shanghai, China, October.
Yousefi, A.M., Lim, J.B.P., Uzzaman, A., Lian, Y., Clifton, G.C. and Young, B. (2017), "Web crippling strength of cold-formed stainless steel lipped channels with web perforations under end-two-flange loading", *Adv. Struct. Eng*.
DOI: 10.1177/1369433217695622
Zhao, O., Gardner, L. and Young, B. (2016), "Buckling of ferritic stainless steel members under combined axial compression and bending", *J. Constr. Steel Res*., **117**, 35-48.
Zhou, F. and Young, B. (2006), "Yield line mechanism analysis on web crippling of cold-formed stainless steel tubular sections under two-flange loading", *Eng. Struct*., **28**(6), 880-892.
Zhou, F. and Young, B. (2007), "Cold-formed high-strength stainless steel tubular sections subjected to web crippling", *J. Struct. Eng*., **133**(3), 368-377.
Zhou, F. and Young, B. (2008), "Web crippling of cold-formed stainless steel tubular sections", *Adv. Struct. Eng*., **11**(6), 679-691.
Zhou, F. and Young, B. (2013), "Web crippling behaviour of cold-formed duplex stainless steel tubular sections at elevated temperatures", *Eng. Struct*., **57**, 51-62.

Nomenclature

A	Web opening ratio;
a	Diameter of circular web opening;
b_f	Overall flange width of section;
b_l	Overall lip width of section;
COV	Coefficient of variation;
d	Overall web depth of section;
E	Young's modulus of elasticity;
h	Depth of the flat portion of web;
L	Length of the specimen;
N	Length of the bearing plate;
P_{ASCE}	Nominal web crippling strength obtained from American Code;
$P_{\mathrm{AS/NZS}}$	Nominal web crippling strength obtained from Australian/New Zealand Code;
P_{FEA}	Web crippling strength per web predicted from finite element (FEA);
P_{NAS}	Nominal web crippling strength obtained from North American Specification;
P_m	Mean value of analysed-to-predicted load ratio;
R	Reduction factor;
R_{P}	Proposed reduction factor;
r_{i}	Inside corner radius of section;
θ	Angle between web and bearing surface
t	Thickness of section;
V_P	Coefficient of variation of Analysed-to-predicted load ratio;
x	Horizontal clear distance of the web openings to the near edge of the bearing plate;
β	Reliability index;